Molecular paneling of *rac*-1,1′-bi-2-naphthol/∼ate (BINOL/BINOLAT): hydrogen-bonded assembly of $[M(NH_3)_{4\ or\ 6}]^{2+}$ complexes (M = Ni, Zn, Cd) in cavities of $\{[BINOLAT]^{2-}(BINOL)_2\}$-strands

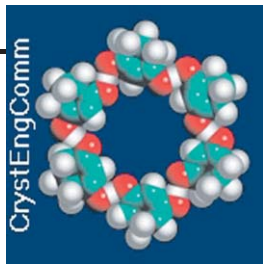

Communication

Barbara Paul,[a] Christian Näther,[b] Bernhard Walfort,[c] Katharina M. Fromm,[d] Boris Zimmermann,[a] Heinrich Lang[c] and Christoph Janiak*[a]

[a]*Institut für Anorganische und Analytische Chemie, Universität Freiburg, Albertstr. 21, D-79104 Freiburg, Germany. E-mail: janiak@uni-freiburg.de; Fax: 49 761 2036147; Tel: 49 761 2036127*

[b]*Institut für Anorganische Chemie, Universität Kiel, Olshausenstr. 40, 24098 Kiel, Germany*

[c]*Institut für Anorganische Chemie, TU Chemnitz, Straße der Nationen 62, D-09111 Chemnitz, Germany*

[d]*Department of Chemistry, University of Basel, Spitalstrasse 51, CH-4056 Basel, Switzerland*

Received 16th July 2004, Accepted 25th August 2004
First published as an Advance Article on the web 3rd September 2004

The naphthyl-paneled cavities in the $\{[BINOLAT]^{2-}(BINOL)_2\}$-host strands in the structures of $[M(NH_3)_n]^{2+}[BINOLAT]^{2-}(BINOL)_2$ accommodate the $[M(NH_3)_n]^{2+}$-guest cation through second-sphere N–H···O hydrogen bonding irrespective of the size (M = Ni or Cd, n = 6) or coordination polyhedron (tetrahedron for M = Zn, n = 4 or octahedron for M = Ni, Cd).

One aspect of crystal engineering is the predictable assembly of supramolecular systems[1,2] such as organic molecular solids and metal coordination compounds (coordination polymers).[3–6] Pre-orientation of one type of building block by metal coordination[7] in combination with second-sphere coordination is a strategy for the design of supramolecular architectures. Second-sphere coordination means the interaction between already coordinatively saturated metal complexes and external ligands, *e.g.* through hydrogen bonding.[8,9] Some biochemical systems utilize second-sphere coordination for the modification of the chemistry around metal ions.[10,11] As a prerequisite for second-sphere coordination, functional groups must be present on the first-sphere ligand which do not coordinate to the metal center but bind the external second-sphere ligands. We have recently reported on the second-sphere coordination of metal complexes with the ligands BEBP[12,13] or DABP[14–17] to anions and crown ethers through N–H···X hydrogen bonding from the amide or amino groups, respectively. Only the bipyridine nitrogen atoms but not the amino groups were found capable of coordinating to a metal ion, yielding the primary complex, *e.g.* $[M(DABP)_3]^{2+}$. This complex can then serve as a building block for larger supramolecular assemblies with the free amino groups as good hydrogen bond donors.

In the supramolecular compound $[Fe^3(DABP)_3]^{2+}[Fe^2(DABP)_3 \subset Fe^1(DABP)_3(nitrophenolate)_6]^{2-}$ the favorable pre-organized conformation of the first sphere complex $[Fe^1(DABP)_3]^{2+}$ is extended with six nitrophenolate H-bond acceptors to create a cavity which is filled through self-inclusion[18] of a crystallographically independent $[Fe^2(DABP)_3]^{2+}$-cation (Scheme 1).[15]

Here we report on the supramolecular organization of *rac*-1,1′-bi-2-naphthol (BINOL) and its dianion ($BINOLAT^{2-}$) through the second-sphere hydrogen-bonding interaction from metal ammin complexes $[M(NH_3)_n]^{2+}$ (Scheme 1).

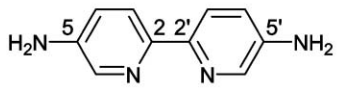

DABP = 5,5'-diamino-2,2'-bipyridine

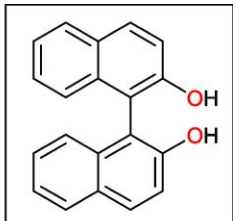

BINOL = *rac*-1,1'-bi-2-naphthol

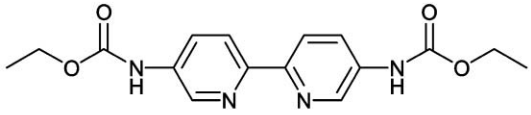

BEBP = 5,5'-bis(ethoxycarbonylamino)-2,2'-bipyridine

Crystals of $[M(NH_3)_n]^{2+}[BINOLAT]^{2-}(BINOL)_2$ (M = Ni, n = 6; Zn, n = 4; Cd, n = 6) could be grown from a 1 : 1 mixture of the metal nitrate and BINOL (0.1 mmol each) in aqueous ammonia–methanol or ethanol.† Increasing the amounts or using a 1 : 3 ratio of M : BINOL led to problems in crystal growth such that crystals of BINOL started to form.

The presence of ammin *versus* aqua ligands on the metal was evident from elemental analysis and proven by simultaneous differential thermoanalysis, thermogravimetry and mass spectrometry (DTA-TG-MS).‡ In addition, this analysis illustrates the (similar) thermal behavior of the compounds. The TG and DTG curves show three mass losses, all of them are accompanied with endothermic events in the DTA curves (Fig. 1). The first TG step (peak temperature: M = Ni, T_p = 195 °C; M = Zn two TG steps, T_p = 93 and 131 °C; M = Cd, T_p = 116 °C) matches with the loss of all ammin ligands (MS-trend-scan m/z = 17; M = Ni, Δm_{exp}: 9.4, Δm_{theo}: 10.0%; M = Zn, Δm_{exp}: 6.4, Δm_{theo}: 6.9%; M = Cd, Δm_{exp}: 6.3, Δm_{theo}: 6.4%;). In the next TG step (M = Ni, T_p = 302 °C; M = Zn, T_p = 302 and 410 °C; M = Cd, T_p = 302 °C) the two free BINOL molecules (m/z = 286) are lost (M = Ni, Δm_{exp}: 48.3,

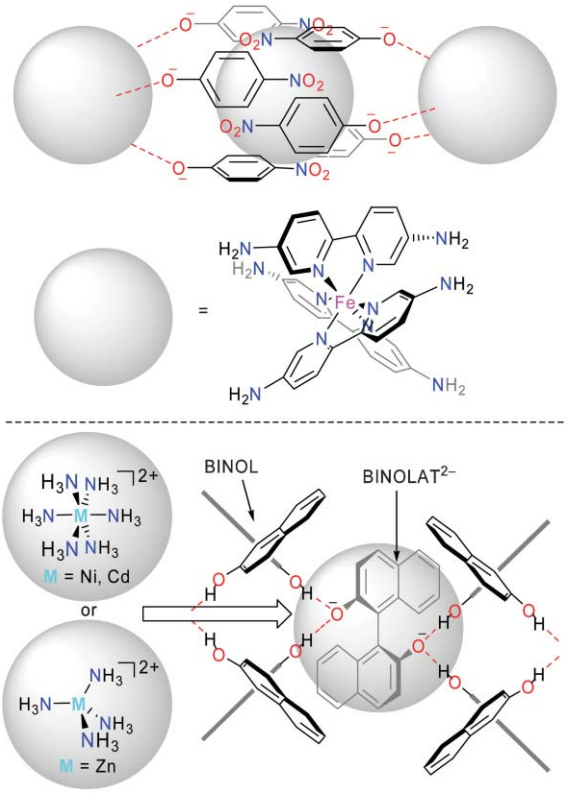

Scheme 1 Top: Cleft formation and molecular paneling based on metal complexes with 5,5′-diamino-2,2′-bipyridine ligands and nitrophenolate H-bond acceptors. Bottom: Hydrogen-bonding arrangement and molecular paneling in the structures of $[M(NH_3)_n]^{2+}[BINOLAT]^{2-}(BINOL)_2$.

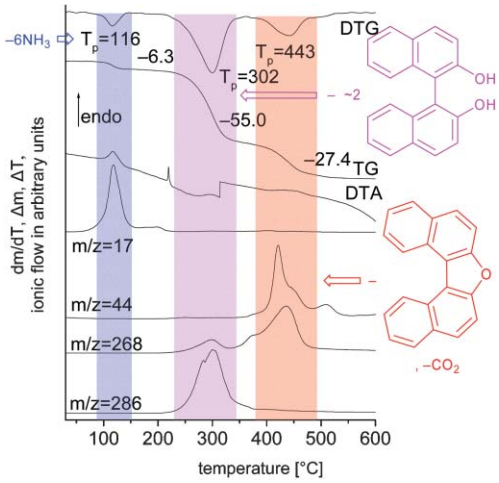

Fig. 1 DTG, TG, DTA and MS-trend-scan curve for $[Cd(NH_3)_6]^{2+}[BINOLAT]^{2-}$ $(BINOL)_2$ (m/z = 17: NH_3, m/z = 44: CO_2, m/z = 268: dinaphthofuran and m/z = 286: BINOL); values refer to the mass loss in % (TG) and to the peak temperature (T_p) in °C (DTG).

Δm_{theo}: 54.5%; M = Zn, Δm_{exp}: 55.0, Δm_{theo}: 56.0%; M = Cd, Δm_{exp}: 55.0, Δm_{theo}: 54.9%). The last TG event (M = Ni, T_p = 454 °C; M = Zn, T_p = 493 °C; M = Cd, T_p = 443 °C) matches with the simultaneous loss of BINOLAT as BINOLAT–O^{2-}, m/z = 268, equivalent to its derivative dinaphtho[1,2-*b* : 1′,2′-*d*]furan[19] and carbon dioxide (m/z = 44) (M = Ni, Δm_{exp}: 24.5, Δm_{theo}: 26.5%; M = Zn, Δm_{exp}: 22.0, Δm_{theo}: 27.1%; M = Cd, Δm_{exp}: 27.4, Δm_{theo}: 25.0%; calc. values are for the furan only, *i.e.* without CO_2). The CO_2 may be formed by partial oxidation of BINOLAT. The intensity of the peaks in the mass spectra do not allow for a measure of the relative amounts of dinaphthofuran and CO_2.

The three compounds $[M(NH_3)_n]^{2+}[BINOLAT]^{2-}(BINOL)_2$ (M = Ni, n = 6; Zn, n = 4; Cd, n = 6) are isostructural.§ The octahedral (M = Ni, Cd) or tetrahedral (M = Zn) ammin-metal environment in the first-sphere complexes $[M(NH_3)_n]^{2+}$ is typical and will not be detailed any further here. The octahedrally coordinated metal atoms sit on a C_2-axis as a special position of the space group $C2/c$. The C_2-axis runs

Table 1 Crystal data and structure refinement for $[M(NH_3)_n]^{2+}[BINOLAT]^{2-}(BINOL)_2$

Compound	M = Ni, n = 6	M = Zn, n = 4	M = Cd, n = 6
Empirical formula	$C_{60}H_{58}N_6NiO_6$	$C_{60}H_{52}N_4O_6Zn$	$C_{60}H_{58}CdN_6O_6$
M/g mol^{-1}	1017.83	990.43	1071.52
Crystal size/mm	0.45 × 0.3 × 0.2	0.4 × 0.3 × 0.3	0.4 × 0.3 × 0.3
θ range/°	2.73–27.23	2.26–27.11	2.87–27.91
H; k; l range	−31, 29; 0, 15; 0, 21	−34, 29; 0, 15; 0, 21	−31, 30; 0, 15; 0, 21
Crystal system	Monoclinic	Monoclinic	Monoclinic
Space group	$C2/c$	$C2/c$	$C2/c$
a/Å	25.272(7)	27.240(5)	25.509(16)
b/Å	12.269(4)	12.519(2)	12.280(8)
c/Å	17.068(5)	17.268(3)	17.201(10)
β/°	110.10(1)	121.2(4)	110.10(2)
V/Å^3	4970(2)	5037(2)	5060(5)
Z	4	4	4
D_{calc}/g cm^{-3}	1.360	1.306	1.406
F(000)	2144	2072	2224
M/mm^{-1}	0.451	0.544	0.492
Max/min transmission	0.99999/0.79165	0.99999/0.32876	0.99999/0.39227
Reflections collected	20697	29420	25593
Unique reflections (R_{int})	5339 (0.0561)	5402 (0.0470)	5469 (0.0462)
Observed reflections [$I > 2\sigma(I)$]	3623	3487	4252
Parameters refined	341	351	341
Max./min. $\Delta\rho$ [a]/e Å^{-3}	0.202/−0.305	1.238/−0.333	0.287/−0.459
R_1/wR_2 [$I > 2\sigma(I)$] [b]	0.0419/0.0909	0.0742/0.2252	0.0332/0.0822
R_1/wR_2 (all data) [b]	0.0710/0.1008	0.1035/0.2518	0.0467/0.0871
Goodness-of-fit on F^2 [c]	1.012	1.035	1.038
Weighting scheme w; a/b [d]	0.0381/3.7392	0.1727/1.1015	0.0413/3.7777

[a] Largest difference peak and hole. [b] $R_1 = [\Sigma(||F_o| - |F_c||)/\Sigma|F_o|]$; $wR_2 = [\Sigma[w(F_o^2 - F_c^2)^2]/\Sigma[w(F_o^2)^2]]^{1/2}$. [c] Goodness-of-fit = $[\Sigma[w(F_o^2 - F_c^2)^2]/(n-p)]^{1/2}$. [d] $w = 1/[\sigma^2(F_o^2) + (aP)^2 + bP]$ where $P = (\max(F_o^2 \text{ or } 0) + 2F_c^2)/3$.

Table 2 Hydrogen bonding interactions in $[M(NH_3)_n]^{2+}[BINOLAT]^{2-}(BINOL)_2$[a]

D–H···A	D–H/Å	H···A/Å	D···A/Å	D–H···A/°	Sym. rel.
M = Ni, n = 6					
Intra-strand BINOL···BINOLAT:					
O1–H10···O3	0.97(3)	1.62(3)	2.567(2)	164(3)	1_545
O2–H20···O3	0.91(3)	1.64(3)	2.527(2)	165(3)	5_566
Ni–NH_3···BINOL/BINOLAT:					
N1–H1A···O1	0.89	2.25	3.075(3)	154	2_556
N1–H1C···O2	0.89	2.58	3.286(3)	137	6_556
N3–H3A···O2	0.89	2.38	3.131(3)	142	6_556
N3–H3C···O3	0.89	2.22	3.086(3)	164	1_545
M = Zn, n = 4					
Intra-strand BINOL···BINOLAT:					
O2–H20···O3	1.13(4)	1.49(4)	2.591(3)	164(3)	2_755
O1–H10···O3	0.99(5)	1.54(5)	2.504(3)	164(4)	6_566
Zn–NH_3···BINOL/BINOLAT:					
N1–H1B···O2	0.89	2.40	3.184(4)	148	
N2–H2A···O1	0.89	2.38	3.239(16)	164	6_565
N2–H2A···O3	0.89	2.58	3.28(2)	136	
N2–H2C···O2	0.89	2.16	2.995(14)	156	
N3–H3C···O1	0.89	2.28	3.03(2)	141	5_766
M = Cd, n = 6					
Intra-strand BINOL···BINOLAT:					
O1–H10···O3	0.84(3)	1.73(3)	2.550(2)	162(3)	1_556
O2–H20···O3	0.85(3)	1.76(3)	2.585(2)	163(3)	5_666
Cd–NH_3···BINOL/BINOLAT:					
N1–H1A···O2	0.89	2.32	3.079(3)	143	
N1–H1C···O1	0.89	2.44	3.216(3)	146	5_667
N2–H2A···O1	0.89	2.38	3.133(3)	142	5_667
N2–H2C···O3	0.89	2.23	3.115(3)	170	6_566

[a] D = donor, A = acceptor. For found and refined atoms the standard deviations are given. Principal symmetry relations (without translation): 1 = x, y, z; 2 = $-x$, y, $-z$ + 1/2; 5 = $-x$, $-y$, $-z$; 6 = x, $-y$, z − 1/2.

through opposite edges of the MN_6-octahedron. The $Zn(NH_3)_4$-tetrahedron is disordered within the naphthyl-paneled cavity (see below) to give a pseudo-trigonal–bipyramidal structure with one of the nitrogen atoms (N4) lying on the C_2-axis (Fig. 2).

The packing of the molecular building blocks in $[M(NH_3)_n]^{2+}[BINOLAT]^{2-}(BINOL)_2$ appears to be controlled by the O–H···O hydrogen bonding between BINOL and BINOLAT (Table 2). Each naphthoxide oxygen atom of the completely deprotonated 1,1′-bi-2-naphtholate moiety (BINOLAT) is an acceptor of two hydrogen bonds from an OH group of each of the two 1,1′-bi-2-naphthol molecules. This hydrogen-bonding mode gives rise to a BINOLAT/BINOL strand formation along c (Fig. 3a). These strands are the same for the different sizes (Ni *versus* Cd in $[M(NH_3)_6]^{2+}$) and shapes (tetrahedral *versus* octahedral) of the metal–ammin cation. The intra-strand naphthyl arrangement exhibits only C–H···π interactions.[20] There is no π–π stacking.[21]

Cavities are created within this BINOLAT/BINOL strand

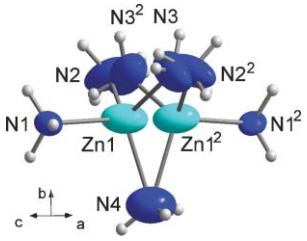

Fig. 2 Disorder of the $Zn(NH_3)_4$-tetrahedron (see text); symmetry relation[2] = $-x$ + 2, y, $-z$ + 1/2.

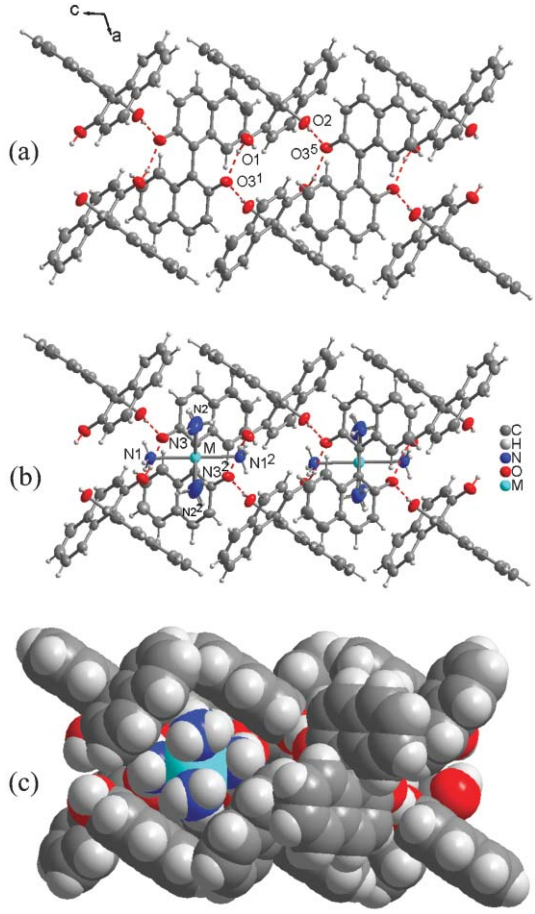

Fig. 3 $[M(NH_3)_n]^{2+}[BINOLAT]^{2-}(BINOL)_2$ structures (M = Ni, Cd, n = 6; M = Zn, n = 4) (a) BINOLAT/BINOL strand arrangement along c with cavity formation through the naphthyl panels. The naphthyl planes of BINOLAT are facing the viewer, those of BINOL are close to perpendicular to the projection plane. Click here to access a 3D view of Fig. 3a. (b) Cavities filled with a $[M(NH_3)_n]^{2+}$ unit. The N–H···O hydrogen bonding is not shown for clarity. (c) Space-filling representation of (b). Click here to access a 3D view of Fig. 3b. Pictures are based on the crystal data of the cadmium compound. For symmetry labels see Table 2.

through the paneling of the naphthyl rings. The cavities are alternatingly located to the front and rear of the strand (Fig. 3). The cavities contain the $[M(NH_3)_n]^{2+}$ fragments (Fig. 3b and c) which are connected with the BINOLAT/BINOL strand through N–H···O hydrogen bonding (see Table 2). The disorder of the $[Zn(NH_3)_4]^{2+}$-tetrahedron (see Fig. 2) in the $[Zn(NH_3)_4]^{2+}[BINOLAT]^{2-}(BINOL)_2$-structure may lend further support to the control of O–H···O hydrogen bonding between BINOL and BINOLAT in the crystal packing because the tetrahedron, unlike the octahedron, is not well suited to fit into the spanned cavity. However, it could also be argued that crystallization had occurred from $[Zn(NH_3)_6]^{2+}$-octahedra available in solution in equilibrium with the $[Zn(NH_3)_4]^{2+}$-tetrahedra. In the final crystalline state two NH_3 ligands were then lost from the unstable $[Zn(NH_3)_6]$-octahedron to yield the more stable tetrahedron. This being the case, the $[M(NH_3)_6]^{2+}$-octahedron would also be a structure determining building block.

The outside of the strands is hydrophobic/lipophilic and neighboring strands are hexagonally close-packed along a and b with the inter-strand packing dictated by C–H···π interactions (Fig. 4).[20]

Each strand contains both enantiomeric forms of the racemic BINOL mixture. For both the BINOLAT and the BINOL moiety the R and S enantiomer alternate along the strand in the

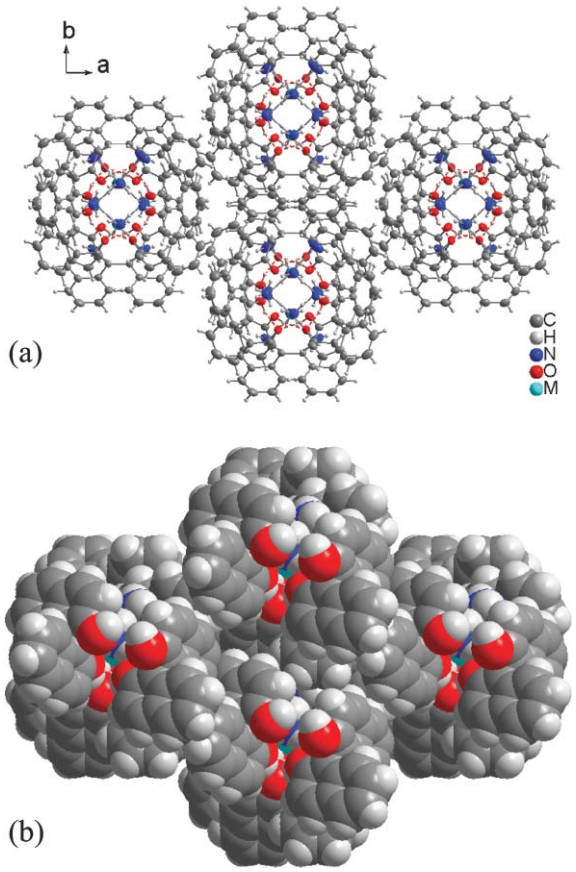

Fig. 4 Inter-strand packing in the structures of $[M(NH_3)_n]^{2+}[BINOLAT]^{2-}(BINOL)_2$ along *a* and *b* with the strands viewed along *c*. (a) Ball-and-stick representation; (b) Space-filling representation of (a). Click here to access a 3D view of Fig. 4a.

c-direction. Work using a single enantiomer for the construction of the $[M(NH_3)_n]^{2+}[BINOLAT]^{2-}$ structures is in progress in the search of enantiomerically pure 1D single-stranded helical molecular networks.[22]

The very similar emission spectra¶ of the supramolecular compounds $[M(NH_3)_n]^{2+}[BINOLAT]^{2-}(BINOL)_2$ show two maxima at 303 and 399 nm (Fig. 5). The maximum at 303 nm is a vibronic side band for the S_0–S_1 system. The maximum at 399 nm is close to the main maxima of 379 and 389 nm in BINOL so that the luminescence is assigned to intraligand transitions.

Support by DFG grant Ja 466/10-2 is appreciated. We thank Prof. Dr Claude Piguet (University of Geneva) for helpful discussions.

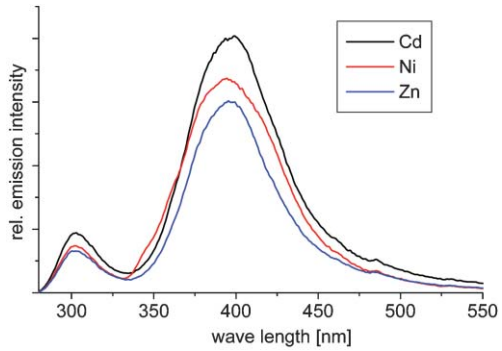

Fig. 5 Emission spectra of $[M(NH_3)_n]^{2+}[BINOLAT]^{2-}(BINOL)_2$ (M = Ni^{2+}, n = 6; Zn^{2+}, n = 4; Cd^{2+}, n = 6) with λ_{exc} = 240 nm.

Notes and References

† General experimental procedure for the preparation of $[M(NH_3)_n]^{2+}[BINOLAT]^{2-}(BINOL)_2$ (M = Ni^{2+}, n = 6; Zn^{2+}, n = 4; Cd^{2+}, n = 6): $M(NO_3)_2{\cdot}(H_2O)_n$ (0.10 mmol, Ni^{2+}, n = 2; Zn^{2+}, n = 4; M = Cd^{2+}, n = 4) in an aqueous solution of ammonia (26%, 5 ml) was combined with a solution of 1,1′-bi-2-naphthol (BINOL, 0.10 mmol, 28.6 mg) in ROH (5 ml, R = Me for M = Cd^{2+}, Zn^{2+}; R = Et for M = Ni^{2+}). The solvent was then allowed to evaporate slowly at room temperature. After several days crystals formed which were suitable for single crystal X-ray diffration. M = Ni: very pale violet blocks, yield 12.0 mg, 35% based on BINOL. $C_{60}H_{58}NiN_6O_6$ (1017.83): calc. C 70.80, H 5.74, N 8.26; found C 70.55, H 5.74, N 8.23%. M = Zn: Colorless blocks, yield 14.6 mg, 43% based on BINOL. $C_{60}H_{52}ZnN_4O_6$ (990.43): calc. C 72.76, H 5.29, N 5.66; found C 70.88, H 5.37, N 5.56%. M = Cd: Colorless needles, yield 11.0 mg, 35% based on BINOL. $C_{60}H_{58}CdN_6O_6$ (1071.52): calc. C 67.25, H 5.46, N 7.84; found C 66.90, H 5.43, N 7.53%. IR and ^1H NMR (DMSO-d_6 + HCl/H_2O because of solubility for M = Ni, Zn) spectra correspond to BINOL with some broadening of the bands between 3250–3500 and slight differences in the fingerprint region in the IR.

‡ TG/MS instrumentation: STA-409CD with skimmer coupling from Netzsch, quadrupole mass spectrometer QMA 400 from Balzers. The MS measurements were performed in analog and trend scan mode. All measurements were corrected for buoyancy and current effects and were performed using heating rates of 4 °C min^{-1} in Al_2O_3 crucibles in a dynamic helium atmosphere (purity 4.6; flow-rate: 75 ml min^{-1}). The thermobalance was calibrated using standard reference materials. Initial mass: M = Ni: 18.27 mg; M = Zn: 17.34 mg; M = Cd: 19.49 mg.

§ X-ray crystallography: *data collection*: Bruker AXS with CCD area-detector, temperature 298(2) K, Mo Kα radiation (λ = 0.71073 Å), graphite monochromator, ω-scans, data collection and cell refinement with SMART,[23] data reduction with SAINT,[23] experimental absorption correction with SADABS.[24] *Structure analysis and refinement*: The structures were solved by direct methods (SHELXS-97);[25] refinement was done by full-matrix least squares on F^2 using the SHELXL-97 program suite.[25] All non-hydrogen positions were found and refined with anisotropic temperature factors. Hydrogen atoms on carbon were calculated (AFIX 43, U(H) = 1.2 U_{eq}(C). Hydrogen atoms of the ammin ligands were located in the difference map but were idealised (d_{N-H} = 0.89 Å), then refined as rigid groups using isotropic displacement parameters (U_{eq} = 1.5 U_{eq}(N)) allowed to rotate but not tip (AFIX 137). Alcoholic hydrogen atoms were located in the difference map and were refined with varying coordinates and varying isotropic displacement parameters. Details of the X-ray structure determinations and refinements are provided in Table 1. Graphics were drawn with DIAMOND.[26] Displacement ellipsoids are drawn at the 50% probability level and H atoms are shown as spheres of arbitrary radii. CCDC reference numbers 244951–244953 for the Zn, Ni and Cd compound, respectively. See http://www.rsc.org/suppdata/ce/b4/b410933c/ for crystallographic data in CIF fomat.

¶ Emission spectra were measured on a Perkin-Elmer LS-50B, λ_{exc} = 240 nm, split widths (em, ex) 5.0 nm, scan speed 2 nm s^{-1}, solid sample in quartz capillary at room temperature.

1 D. Braga, *Chem. Commun.*, 2003, 2751.
2 D. Braga, G. R. Desiraju, J. S. Miller, A. G. Orpen and S. L. Price, *CrystEngComm*, 2002, **4**, 500.
3 K. Biradha, *CrystEngComm*, 2003, **5**, 374.
4 C. Janiak, *Dalton Trans.*, 2003, 2781.
5 S. L. James, *Chem. Soc. Rev.*, 2003, **32**, 276.
6 C. B. Aakeröy and A. M. Beatty, *Compr. Coord. Chem. II*, 2003, **1**, 679.
7 M. Fujita, *Struct. Bond.*, 2000, **96**, 177.
8 L. Brammer, *Dalton Trans.*, 2003, 3145.
9 A. M. Beatty, *CrystEngComm*, 2001, **51**, 1.
10 S. J. Loeb, in *Comprehensive Supramolecular Chemistry*, ed. J. L. Atwood, J. E. D. Davies, D. D. MacNicol and F. Vögtle, Elsevier Science, New York, 1996, vol. 1, 733.
11 F. M. Raymo and J. F. Stoddart, *Chem. Ber.*, 1996, **129**, 981; H. M. Colquhoun, J. F. Stoddart and D. J. Williams, *Angew. Chem., Int. Ed. Engl.*, 1986, **25**, 487; M. Botta, *Eur. J. Inorg. Chem.*, 2000, 399; K. Zamaraev, *New J. Chem.*, 1994, **18**, 3; J. W. Steed, *Coord. Chem. Rev.*, 2001, **215**, 171; Z. Shirin, J. Thompson, L. Liable-Sands, G. P. A. Yap, A. L. Rheingold and A. S. Borovik, *J. Chem. Soc., Dalton Trans.*, 2002, 1714.
12 B. Wu, X.-J. Yang, C. Janiak and P.-G. Lassahn, *Chem. Commun.*, 2003, 902.
13 X.-J. Yang, C. Janiak, J. Heinze, F. Drepper, P. Mayer, H. Piotrowski and P. Klüfers, *Inorg. Chim. Acta*, 2001, **318**, 103.

14 C. Janiak, S. Deblon, H.-P. Wu, M. J. Kolm, P. Klüfers, H. Piotrowski and P. Mayer, *Eur. J. Inorg. Chem.*, 1999, 1507.
15 X.-J. Yang, B. Wu and C. Janiak, *CrystEngComm*, 2004, **6**, 126.
16 X.-J. Yang, B. Wu, W.-H. Sun and C. Janiak, *Inorg. Chim. Acta*, 2003, **343**, 366.
17 X.-J. Yang, B. Wu, C. Janiak, W.-H. Sun and H.-M. Hu, *Z. Anorg. Allg. Chem.*, 2004, **630**, 1564.
18 S. Aitipamula, G. R. Desiraju, M. Jaskólski, A. Nangia and R. Thaimattam, *CrystEngComm*, 2003, **5**, 447, and references therein.
19 E. Armengol, A. Corma, H. Garcia and J. Primo, *Eur. J. Org. Chem.*, 1999, **8**, 1915.
20 M. Nishio, *CrystEngComm*, 2004, **6**, 130; M. Nishio, M. Hirota and Y. Umezawa, *The CH/π interaction (evidence, nature and consequences)*, Wiley-VCH, 1998; Y. Umezawa, S. Tsuboyama, K. Honda, J. Uzawa and M. Nishio, *Bull. Chem. Soc. Jpn.*, 1998, **71**, 1207; C. Janiak, S. Temizdemir, S. Dechert, W. Deck, F. Girgsdies, J. Heinze, M. J. Kolm, T. G. Scharmann and O. M. Zipffel, *Eur. J. Inorg. Chem.*, 2000, 1229.
21 C. Janiak, *J. Chem. Soc., Dalton Trans.*, 2000, 3885.
22 P. Grosshans, A. Jouaiti, V. Bulach, J.-M. Planeix, M. W. Hosseini and J.-F. Nicoud, *CrystEngComm*, 2003, **5**, 414.
23 SMART, Data Collection Program for the CCD Area-Detector System; SAINT, Data Reduction and Frame Integration Program for the CCD Area-Detector System. Bruker Analytical X-ray Systems, Madison, Wisconsin, USA, 1997.
24 G. Sheldrick, Program SADABS: Area-detector absorption correction, University of Göttingen, Germany, 1996.
25 G. M. Sheldrick, SHELXS-97, SHELXL-97, Programs for crystal structure analysis, University of Göttingen, Germany, 1997.
26 DIAMOND 2.1e for Windows, Crystal Impact Gbr, Bonn, Germany, http://www.crystalimpact.com/diamond.